Int. J. Solids Structures Vol. 19, No. 4, pp. 337–355, 1983
Printed in Great Britain.

0020-7683/83/040337-19$03.00/0
Pergamon Press Ltd.

CONTINUUM THEORY OF DILATANT TRANSFORMATION TOUGHENING IN CERAMICS

B. BUDIANSKY, J. W. HUTCHINSON and J. C. LAMBROPOULOS
Division of Applied Sciences, Harvard University, Cambridge, MA 02138, U.S.A.

(*Received* 8 *March* 1982; *in revised form* 6 *July* 1982)

Abstract—A continuum description is introduced for an elastic solid which contains particles that undergo an irreversible stress-induced dilatant transformation. The behaviors of the composite solid considered range from abrupt complete transformation at a critical mean stress to strain controlled transformation at constant stress. It is useful to define and distinguish between super-critically and sub-critically transforming materials. Stress and strain fields in the transformation zone at the tip of a macroscopic crack are determined for stationary and growing cracks. The near-tip stress intensity factor is related to the applied stress intensity factor. Toughening is associated with crack advance and is due to the wake of transformed particles which are left behind a quasi-statically advancing crack-tip. Detailed calculations for the toughening are made over a wide range of possible material parameters.

1. INTRODUCTION

Fracture toughness enhancement has been observed in a number of ceramic systems containing particles which undergo a transformation of the martensitic type[1]. The high stresses in the vicinity of a macroscopic crack induce a transformation of the particles and thereby alter the crack tip stress field in a way which will be studied in this paper. To date, most systems which have been investigated experimentally contain zirconia (ZrO_2) particles embedded in a matrix of nontransforming ceramic. These particles transform from a tetragonal to a monoclinic crystal structure at sufficiently high stress. Were it unconstrained the transformation would involve a shear strain of about 16% and a dilatation of 4%. When embedded in a surrounding elastic matrix a particle is observed to transform into a number of bands with the sense of shear alternating from one band to the next. The *average* shear transformation over the particle is very much less than 16%. On the other hand, the dilatant transformation strain is the same in each band and still averages about 4% over the particle.

McMeeking and Evans[2], taking into account just the dilatant part of the transformation, have predicted increases in toughness which are comparable to, but apparently less than, corresponding experimental values. In this study we too neglect any shear component of the transformation, and we assume that the onset of the dilatant transformation occurs at a critical mean stress. Furthermore, attention is limited to systems with sufficiently small particles and spacing between particles such that the transformation zone at the crack tip spans many particles. Under these circumstances a continuum, or macroscopic, description of the composite system can be used which averages over the matrix and particles.

We have taken over a number of theoretical ideas and methods from elastic–plastic fracture mechanics. While here these are developed within the context of dilatant transformation behavior, some of them may be extended to include distortional transformations. We start in Section 2 by giving the macroscopic behavior of an idealized two-phase composite where the particle phase undergoes a purely dilatant irreversible transformation. The results for this system are then used to motivate the macroscopic stress–strain behavior of the composite material employed in the study. In Section 3 it is shown that enhanced toughness cannot be explained by the transformation zone at the tip of a stationary crack. Increases in toughness are due to transformed particles left behind in the wake of a stably advancing crack tip, and the last three sections of the paper give a detailed analysis of the growing crack. The maximum possible toughness increase due to dilatant transformation is determined and compared with available experimental information. The results of McMeeking and Evans[2] will be placed in perspective with respect to both the material characterization and the perturbing influence of the transformation itself on the size and shape of the transformation zone.

2. CONSTITUTIVE BEHAVIOR OF A SPECIAL TWO PHASE COMPOSITE MATERIAL

Some exact results are given below for a special two component material comprising a linear elastic matrix material with embedded particles which undergo an irreversible inelastic dilatation. The assumed constitutive behavior of the individual particles is not, in general, the same as that of a particle undergoing a true dilatant phase transformation. Nevertheless, the results for this idealized composite do lend insight to what can be expected for a more complicated system.

Each component of the composite is assumed isotropic and we consider the special case in which the particle and matrix have identical linear shear behavior so that in each

$$s_{ij} = 2Ge_{ij} \tag{1}$$

where **s** is the stress deviator, **e** is the strain deviator, and G is the common shear modulus. The matrix material responds linearly under hydrostatic tension and compression with bulk modulus B according to

$$\sigma_m \equiv \frac{1}{3}\sigma_{pp} = B\epsilon_{pp} \tag{2}$$

where $\boldsymbol{\sigma}$ and $\boldsymbol{\epsilon}$ are the stress and strain tensors, σ_m is the mean stress, and ϵ_{pp} is the total dilatation.

The dilatant response of the particles is depicted in Fig. 1. Under monotonically increasing ϵ_{pp}, the particles satisfy (2) with the same bulk modulus B as the matrix material as long as

$$\epsilon_{pp} \leq \sigma_m{}^c/B \tag{3}$$

where $\sigma_m{}^c$ is the critical mean stress associated with the start of transformation. On the intermediate segment of the curve the incremental response is governed by B' according to

$$\dot{\sigma}_m = B'\dot{\epsilon}_{pp}. \tag{4}$$

The inelastic, or transformed, part of the dilatation in the particle is denoted by θ_p and it is defined as the difference between the total dilatation and the linear elastic dilatation, i.e.

$$\theta_p = \epsilon_{pp} - \sigma_m/B. \tag{5}$$

The maximum transformed dilatation in each particle is $\theta_p{}^T$ and thus (4) holds in the interval

$$\frac{\sigma_m{}^c}{B} < \epsilon_{pp} < \frac{\sigma_m{}^c}{B} + \theta_p{}^T\left[1 - \frac{B'}{B}\right]^{-1}. \tag{6}$$

For larger values of ϵ_{pp} the incremental response is again governed by the elastic bulk modulus

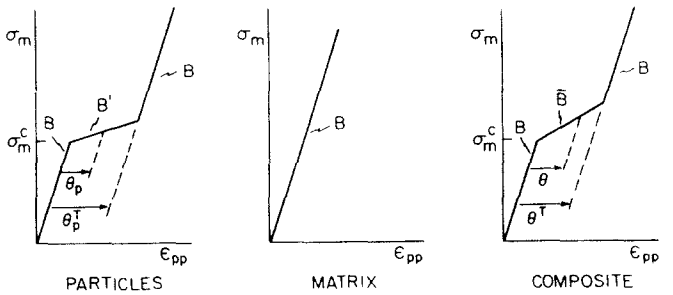

Fig. 1. Dilatant stress–strain behavior of particles and matrix material making up a two-phase composite. The shear behavior is linear with the same shear modulus in both phases. The macroscopic behavior of the composite is also shown.

according to

$$\dot{\sigma}_m = B\dot{\epsilon}_{pp}. \tag{7}$$

The volume fraction of the particles is denoted by c and no assumptions on their shapes need be made. The results quoted below can be derived along the lines given by Hill[3] in his study of the overall moduli of two-phase isotropic elastic composites where both phases have the same shear modulus. (Derivations will not be given here.) The stress–strain behavior to be shown for the composite is exact with the usual interpretation of average, or overall, stress and strain for a multi-phase material.

The shear modulus of the composite is G at all strains and the bulk modulus B governs for $\epsilon_{pp} \leq \sigma_m^c/B$ and again, incrementally, at sufficiently large ϵ_{pp} as shown in Fig. 1. Once ϵ_{pp} exceeds σ_m^c/B the response is incrementally linear with

$$\dot{\sigma}_m = \bar{B}\dot{\epsilon}_{pp} \tag{8}$$

where $\bar{B}$ satisfies

$$\frac{1}{\bar{B}+4G/3} = \frac{c}{B'+4G/3} + \frac{1-c}{B+4G/3}. \tag{9}$$

The dilatation is uniform in each particle and is the same in all particles. The overall transformed dilatation of the composite is defined by

$$\theta \equiv \epsilon_{pp} - \sigma_m/B. \tag{10}$$

On the intermediate segment of the curve

$$\theta = (1-\bar{B}/B)(\epsilon_{pp} - \sigma_m^c/B) \tag{11}$$

with the overall and local transformed dilatations related by $\theta = c\theta_p$. The maximum, or complete, transformed dilatation of the composite is

$$\theta^T = c\theta_p^T \tag{12}$$

as shown originally by Crum (Nabarro[4]). The strain range of the intermediate branch is

$$\frac{\sigma_m^c}{B} < \epsilon_{pp} < \frac{\sigma_m^c}{B} + \theta^T\left[1-\frac{\bar{B}}{B}\right]^{-1}. \tag{13}$$

For ϵ_{pp} increased above the upper limit in (13) no further transformation occurs and (7) applies. If at any strain level beyond σ_m^c/B the dilatation starts to decrease, the transformed dilatation in the particles is frozen and the incremental unloading response is governed by B.

Equation (9) for $\bar{B}$ remains valid even for negative B', although this result is not necessarily unique when $B' < -4G/3$. If $B' > -4G/3$, the equations governing the incremental behavior of the particles are elliptic so that the stress and strain fields in the particles are necessarily smooth and unique. If $B' < -4G/3$ the incremental equations are hyperbolic and certain discontinuities in the stress and strain fields in the particles become possible. Furthermore, if $B' \leq -4G/3$ a particle in an infinite elastic matrix with moduli B and G can transform completely to θ_p^T as soon as the critical mean stress is reached. From (9), it is seen that the transition from elliptic to hyperbolic behavior in the particles at $B' = -4G/3$ gives $\bar{B} = -4G/3$, so that the corresponding transition for the composite coincides with that of the particles in this special system.

In the study carried out below we adopt the dilatant stress–strain behavior for the composite shown in Fig. 1 and again in more detail in Fig. 2. It must be emphasized that we are not assuming that the particle response in an actual system is that specified above. Experimen-

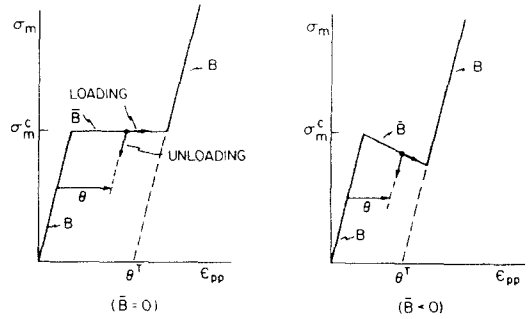

Fig. 2. Dilatant stress-strain behavior of the composite used in the present study.

tal observations suggest that partially transformed states of individual particles do not exist. A given particle is either untransformed or fully transformed. On the other hand, an actual composite system will usually have a distribution of particle sizes with an associated distribution of critical stresses. Thus, even though each particle transforms completely when its own critical stress is attained, a distribution of critical stresses may result in a composite whose incremental bulk modulus never drops below $-4G/3$. Indeed, if the distribution is sufficiently wide it is conceivable that the incremental bulk modulus of the composite might not even become negative.

For the stress-strain behavior in Fig. 2 with $\bar{B} > -4G/3$, it can be shown that the spatial distribution of the macroscopic transformed dilatation θ must be continuous. Thus, in general, there will exist regions in any nonhomogeneously deformed composite in which $\theta < \theta^T$, corresponding to partially transformed macroscopic states. If $\bar{B} \leq -4G/3$, discontinuities in θ can occur, and for the crack problems considered in this paper, the composite does undergo the full macroscopic transformation θ^T as soon as $\sigma_m{}^c$ is attained, and θ jumps from 0 to θ^T across the transformation zone boundary. The condition $\bar{B} > -4G/3$ has additional significance for the incremental behavior of the composite. With $G > 0$, this is the condition for a real longitudinal wave speed. It is also the condition which excludes internal stretching necking modes that can, in principle, develop when ellipticity is lost.

Not only is the physical response of the composite strongly dependent on whether $\bar{B}$ is greater or less than $-4G/3$, the mathematical techniques used to generate solutions to the crack problems posed below also differ depending on whether $\bar{B}$ is above or below this transition. For this reason we introduce the following terminology to distinguish the two ranges of behavior:

$$\begin{aligned}
&\bar{B} > -4G/3 \Leftrightarrow \text{sub-critically transforming composite}\\
&\bar{B} = -4G/3 \Leftrightarrow \text{critically transforming composite}\\
&\bar{B} < -4G/3 \Leftrightarrow \text{super-critically transforming composite.}
\end{aligned} \tag{14}$$

The incremental form of the equations for the composite are analogous to those for an elastic-plastic solid. For any stress state not on the transforming branch

$$\dot{\sigma}_m = B\dot{\epsilon}_{pp} \quad \text{and} \quad \dot{\theta} = 0. \tag{15}$$

On the transforming branch there are two possible incremental responses which will be called loading and unloading, borrowing plasticity terminology. As shown in Fig. 2, loading occurs if $\dot{\epsilon}_{pp} > 0$ and

$$\dot{\sigma}_m = \bar{B}\dot{\epsilon}_{pp} \quad \text{with} \quad \dot{\theta} = (1 - \bar{B}/B)\dot{\epsilon}_{pp}. \tag{16}$$

Unloading occurs if $\dot{\epsilon}_{pp} < 0$ and then (15) applies. Upon unloading to zero mean stress the transformed, or permanent, dilatation is θ. If θ is less than θ^T the material is said to be partially transformed, in the sense described above, while it is called fully transformed when θ attains θ^T. The full transformation θ^T can be identified with $c\theta_p{}^T$.

Given a transformed dilatation θ the integrated stress-strain relations in three-dimensions are

$$\epsilon_{ij} = \frac{1}{2G} s_{ij} + \frac{1}{3B} \sigma_m \delta_{ij} + \frac{1}{3} \theta \delta_{ij} \tag{17}$$

and

$$\sigma_{ij} = 2Ge_{ij} + B(\epsilon_{pp} - \theta)\delta_{ij}. \tag{18}$$

In plane strain ($\epsilon_{33} = \epsilon_{13} = \epsilon_{23} = 0$) the above reduce to

$$\sigma_{\alpha\beta} = 2G\left(\epsilon_{\alpha\beta} - \frac{1}{3}\epsilon_{\mu\mu}\delta_{\alpha\beta}\right) + B(\epsilon_{\mu\mu} - \theta)\delta_{\alpha\beta} \tag{19}$$

$$\sigma_{33} = -\tfrac{2}{3}G\epsilon_{\mu\mu} + B(\epsilon_{\mu\mu} - \theta) \tag{20}$$

$$\sigma_m = \frac{1+\nu}{3}\sigma_{\mu\mu} - \frac{E}{9}\theta \tag{21}$$

and

$$\epsilon_{\alpha\beta} = \frac{1}{2G}(\sigma_{\alpha\beta} - \nu\sigma_{\mu\mu}\delta_{\alpha\beta}) + \frac{(1+\nu)}{3}\theta\delta_{\alpha\beta} \tag{22}$$

where the Greek subscripts range over 1 to 2 with a repeated Greek subscript indicating a sum over just 1 and 2. Here, ν is Poisson's ratio of the elastic branch so that

$$G = \frac{E}{2(1+\nu)} \quad \text{and} \quad B = \frac{E}{3(1-2\nu)} \tag{23}$$

where E is Young's modulus.

3. CRACK TIP STRESS INTENSITY FACTOR FOR A STATIONARY CRACK: APPLICATION OF THE J-INTEGRAL

Throughout this paper it will be assumed that the height of the transformation zone is small compared with the length of the crack. Under this *small scale transformation* condition an asymptotic problem can be formulated for a semi-infinite crack (see Fig. 3) in which the stress field remote from the tip is given by

$$\sigma_{ij} = \frac{K}{\sqrt{(2\pi r)}} f_{ij}(\phi) \qquad (r \to \infty) \tag{24}$$

where K is the elastic stress intensity factor determined for the actual geometry of a cracked specimen at a given load. Here K will be referred to as the applied or remote stress intensity factor. It is the critical value of this K which is determined in a standard fracture toughness test. In this paper attention will be focussed on plane strain crack problems in which the stress

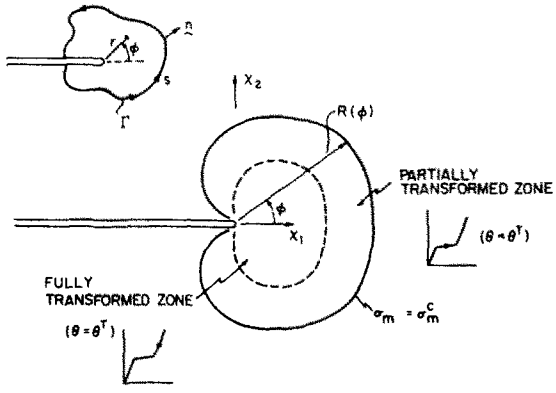

Fig. 3. Small scale transformation problem for stationary crack.

fields are symmetric with respect to the crack (Mode I). Under these circumstances the functions $f_{ij}(\phi)$ are universal and are given in many texts on fracture mechanics. They are defined such that $f_{22}(0) = 1$ so that on the line ahead of the crack the normal stress is

$$\sigma_{22} = K/\sqrt{(2\pi r)}. \tag{25}$$

For cracks in the materials considered here the stresses and strains are unbounded at the crack tip. As the tip is approached the material is fully transformed and the singular behavior is governed by the moduli G and B. Thus, asymptotically as the tip is approached the stress field has precisely the same form as (24) except that the amplitude will in general be different, i.e.

$$\sigma_{ij} = \frac{K_{\text{tip}}}{\sqrt{(2\pi r)}} f_{ij}(\phi) \quad \text{as} \quad r \to 0. \tag{26}$$

It will be assumed that K_{tip} governs the fracture processes at the tip, and therefore it is the reduction from K to K_{tip} which determines the toughening due to transformation.

With no transformation $K_{\text{tip}} = K$. This remains true even in the presence of a transformation zone when there is no crack growth and when K is increased monotonically. The proof of this assertion follows simply from an application of the J-integral of Rice[5]. Under monotonically increasing K it can be reasonably assumed that no unloading occurs anywhere in the transformation zone. That is, ϵ_{pp} increases monotonically at every point as K is increased. If this is the case, the separate unloading response of the material can be disregarded and the material can be thought of as a small strain, nonlinearly elastic solid with the three-segment dilatation curve shown in Fig. 2. The formalism of the J-integral applies. The material is homogeneous with strain-energy density given by

$$W(\boldsymbol{\epsilon}) = \int_0^{\boldsymbol{\epsilon}} \sigma_{ij}\, \mathrm{d}\epsilon_{ij} = \frac{1}{2} G e_{ij} e_{ij} + \int_0^{\epsilon_{pp}} \sigma_m\, \mathrm{d}\epsilon_{pp} \tag{27}$$

and

$$J = \int_\Gamma (W n_1 - \sigma_{ij} n_j u_{i,1})\, \mathrm{ds} \tag{28}$$

where **u** is the displacement vector and **n** is the unit normal to the contour Γ encircling the tip as shown in Fig. 3.

On a contour Γ chosen remote from the tip, J is evaluated on the basis of (24) giving[5]

$$J = (1 - \nu^2) K^2 / E \tag{29}$$

while an identical calculation using (26) for a contour shrunk down around the tip gives

$$J = (1 - \nu^2) K_{\text{tip}}^2 / E. \tag{30}$$

Thus, by path-independence it follows that $K_{\text{tip}} = K$. No assumption regarding the location of the boundary of the transformation zone nor the distribution of θ has had to be made. The assumption that no unloading occurs under monotonically increasing K is equivalent to the condition that ϵ_{pp} increases monotonically as the crack tip is approached on every radial line in this small scale transformation problem. Similar, but more restrictive, conditions for the applicability of the J-integral to elastic–plastic cracked bodies under monotonic loading are also required and have been found to be satisfied to a fairly high degree of accuracy. The standard proof of the path independence of J assumes continuity of the stress and strain fields which only holds for the sub-critically transforming material. However, under the usual assumptions on continuity of tractions and displacements, a generalized definition of J can be made for the super-critically transforming material such that J is still path-independent, and the conclusion that $K_{\text{tip}} = K$ remains intact, as will be shown elsewhere.

4. STRESS INTENSITY CHANGE DUE TO DILATANT SPOTS NEAR A CRACK TIP

A reduction in near-tip stress intensity relative to the applied stress intensity occurs when quasi-static crack advance takes place. Insight into this process is obtained from the following basic solution which is given in Refs. [2, 6]. This solution is the kernel function in the analytic solutions which follow.

Two circular cylindrical "spots" of radius b are symmetrically located with respect to the crack as shown in Fig. 4. We consider the plane strain ($\epsilon_{33} = 0$) deformation which results when each spot undergoes a uniform dilatant transformation θ. From (22) it can be seen that if the spots were subject to no in-plane constraint (i.e. $\sigma_{\alpha\beta} = 0$ with $\epsilon_{33} = 0$) the resulting nonzero strains would be $\epsilon_{11} = \epsilon_{22} = (1 + \nu)\theta/3$. In other words, the transformation θ corresponds to a plane strain transformational area dilatation in the spots of

$$\Omega = \frac{2}{3}(1 + \nu)\theta. \tag{31}$$

The near-tip stress field is of the form (26) and the stress intensity factor induced is [2, 6]

$$\Delta K_{\text{tip}} = \sqrt{\left(\frac{\pi}{8}\right)} \frac{Eb^2\Omega}{(1 - \nu^2)d^{3/2}} \cos\frac{3}{2}\beta. \tag{32}$$

Any transformed material which falls within a 120° fan ahead of the tip (i.e. $\beta < \pi/3$) increases the near-tip intensity, while transformed material behind this fan reduces that intensity. In particular, any transformed material left behind in the wake of an advancing tip will tend to lower the net near-tip intensity, and it is this observation which motivates the study of the growing crack problem given in the next sections.

The basic solution (32) permits the calculation of the near-tip intensity factor if the transformation zone and the distribution of θ within it are known. With K as the remote intensity and with A denoting the region of the transformation zone above $x_2 = 0$, it follows by superposition that

$$K_{\text{tip}} = K + \frac{E}{3\sqrt{(2\pi)}(1 - \nu)} \iint_A \theta r^{-3/2} \cos\frac{3}{2}\phi \, dA. \tag{33}$$

In general neither A nor $\theta(r, \phi)$ is known in advance. While we have already shown that $K_{\text{tip}} = K$ for the stationary crack, it is useful to mention briefly a calculation carried out by McMeeking and Evans [2] for the super-critically transforming material with $\theta = \theta^T$ everywhere in the zone. They approximate the boundary of the transformation zone by using the unperturbed elastic solution (24) to calculate the mean stress which gives

$$\sigma_m = \frac{K(1 + \nu)}{3}\left(\frac{\pi r}{2}\right)^{-1/2} \cos(\phi/2). \tag{34}$$

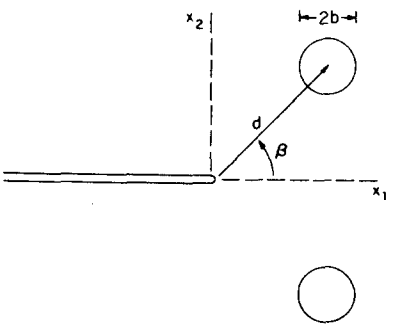

Fig. 4. Symmetrically placed dilatant circular spots at a crack tip.

Equating (34) to σ_m^c, they find

$$R(\phi) = \frac{2}{9\pi}(1+\nu)^2\left(\frac{K}{\sigma_m^c}\right)^2 \cos^2(\phi/2) \tag{35}$$

as the distance to the boundary of A. The double integral in (33) is readily evaluated for this zone shape and is found to be zero. From this calculation alone it can only be concluded that $K_{tip} = K$ to order $(\theta^T)^2$ since (35) rigorously gives the zone boundary only as $\theta^T \to 0$. However, the previous demonstration that $K_{tip} = K$ was free of this restriction.

5. STEADY-STATE, QUASI-STATIC CRACK GROWTH: K_{tip} FOR SUPER-CRITICALLY TRANSFORMING MATERIALS

If it is assumed that crack growth starts and progresses quasi-statically with K_{tip} maintained at a critical value, then the applied intensity factor K must increase with crack advance. Otherwise, the wake of transformed material left behind the advancing tip would reduce the near-tip intensity. By simulating this growth process in the super-critically transforming material, McMeeking and Evans[2] have shown that the applied K must increase with crack advance Δa to produce a resistance curve such as that shown in Fig. 5. Their study shows that K approaches a constant, steady-state value after a relatively small amount of advance amounting to only two or three times the half-height of the transformation zone. In an actual toughness test the steady-state value of K would not be reached because the crack would become unstable and run dynamically at a somewhat lower applied K. The value of K at this point of instability depends on the compliance of the loading device and specimen as well as on the resistance curve itself. But, since the resistance curve has a large initial slope in transforming ceramics, it can be expected that the K at which the crack runs dynamically will generally be close to the steady-state value.

In the remaining sections we present a detailed study of the limiting steady-state problem which is depicted in Fig. 6. This problem supplies the minimum possible value of K_{tip}/K and, correspondingly, the maximum possible toughness enhancement. The crack is imagined to have advanced at constant K leaving behind a semi-infinite wake of half-height H. To an observer moving with the tip, the stress and strain fields remain unchanged.

The boundary of the loading zone in the region ahead of the tip occurs where $\sigma_m = \sigma_m^c$. All stress components are continuous across the boundary when $\bar{B} > -4G/3$, but σ_m experiences a discontinuous drop in a super-critically transforming material element ($\bar{B} \leq -4G/3$) as it passes into the zone. For this material the condition $\sigma_m = \sigma_m^c$ must be attained as the boundary is approached from ahead of the zone. For the sub-critically transforming materials the zone has a region which is only partially transformed ($\theta < \theta^T$) as well as a completely transformed portion ($\theta = \theta^T$) as shown in Fig. 6. Loading occurs in the forward part of the transformation zone where $\dot{\epsilon}_{pp} > 0$, and the rear boundary of the loading zone occurs where $\dot{\epsilon}_{pp} = 0$. Behind this rear

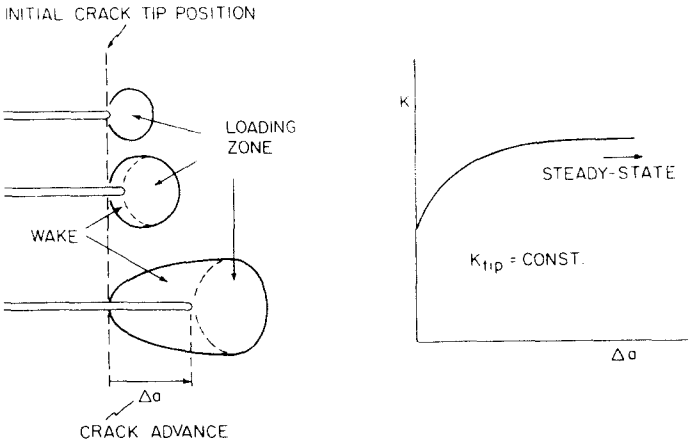

Fig. 5. Transient history of K vs crack advance for growth with K_{tip} maintained constant.

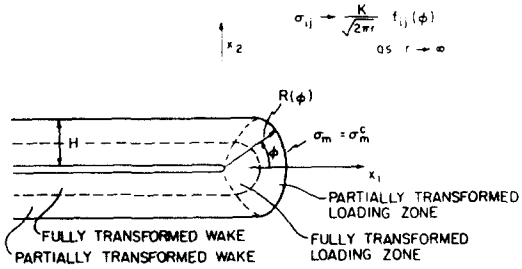

Fig. 6. Steady-state growth under constant K.

boundary, in the region called the wake, the material unloads and no further transformation takes place. Therefore, the distribution of the transformation in the wake is independent of x_1, so that $\theta \equiv \theta(x_2)$ in the wake. Of course, for the super-critically transforming material $\theta = \theta^T$ everywhere in the loading zone and wake.

The next section gives the results of a finite element analysis of the steady-state problem for sub-critically transforming materials. In this section, results for the super-critically transforming material are presented. We start by deriving an asymptotic result valid for sufficiently small θ^T.

Asymptotically for sufficiently small θ^T, the size and shape of the transformation zone can be found from the elastic solution. The condition $\sigma_m = \sigma_m{}^c$ for the front edge of the zone again gives (35) when the elastic solution (34) is used. The wake boundary ($x_2 = H$) merges with the leading zone boundary at the point on (35) corresponding to its maximum height above the x_1-axis where its tangent is horizontal. This occurs where

$$\phi_0 = \pi/3 \quad (60°) \tag{36}$$

and the resulting estimate for the boundary of the entire upper half of the zone can be written as

$$R(\phi) = \frac{8}{3\sqrt{(3)}} H \cos^2 \frac{\phi}{2} \quad 0 \le \phi \le \phi_0 \tag{37}$$

$$= H/\sin \phi \qquad \phi_0 \le \phi \le \pi \tag{38}$$

where the half-height of the wake is

$$H = \frac{\sqrt{(3)}(1+\nu)^2}{12\pi} \left(\frac{K}{\sigma_m{}^c}\right)^2. \tag{39}$$

With $\theta = \theta^T$, the integrations required for evaluation of K_{tip} in (33) can be carried out analytically. (The simplest procedure is to integrate first with respect to x_1 from $-\infty$ to the leading edge of the zone and then integrate with respect to x_2 from 0 to H.) The result is

$$K_{tip} = K - \frac{E\theta^T}{(1-\nu)} \frac{1}{2} \left(\frac{H}{\sqrt{(3)}\pi}\right)^{1/2}$$

$$= K - 0.2143 \frac{E\theta^T \sqrt{(H)}}{(1-\nu)} \tag{40}$$

in agreement with the result of McMeeking and Evans[2], who used numerical integration and a somewhat different approach to obtain their result. By eliminating H using (39), one can also write

$$\frac{K_{tip}}{K} = 1 - \frac{3\sqrt{(3)}}{8} \alpha \tag{41}$$

where α is an important nondimensional parameter which will appear again and which is given by

$$\alpha = \frac{2(1+\nu)E\theta^T}{9\pi(1-\nu)\sigma_m{}^c} \qquad (\theta^T = c\theta_p{}^T). \tag{42}$$

In the remainder of this section we present numerical results for the super-critically transforming materials when α is not restricted to be small. Details of the calculation are given in the Appendix. For arbitrary values of α the zone is no longer given by (37)–(39). The numerical solution involves an iterative procedure for determining the zone boundary. Once it is found, K_{tip} is evaluated using (33). To a very good approximation, the shape remains described by (37) and (38) but the half-height H of the zone is less than the prediction (39) when α is not small. The computed half-height is normalized by the r.h.s. of (39) and plotted as a function of α in Fig. 7. The computed ratio K_{tip}/K as a function of α is the lowest of the solid line curves in Fig. 8. There it can be seen that the asymptotic formula (41), which is plotted as a dashed line, underestimates K_{tip}/K. A plot of K_{tip}/K as a function of the dimensionless parameter $E\theta^T\sqrt{(H)}/[(1-\nu)K]$ is shown in Fig. 9, where the lowest solid line curve again applies to the super-critically transforming materials. For this relationship the simple asymptotic equation (40) provides an excellent approximation over the full range computed, as was conjectured by McMeeking and Evans[2]. The other solid line curves in Figs. 8 and 9 apply to the sub-critically transforming materials, which will be discussed next.

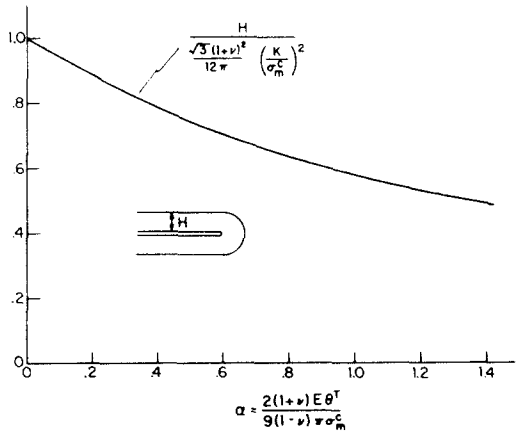

Fig. 7. Half-height of transformation zone for super-critically transforming materials.

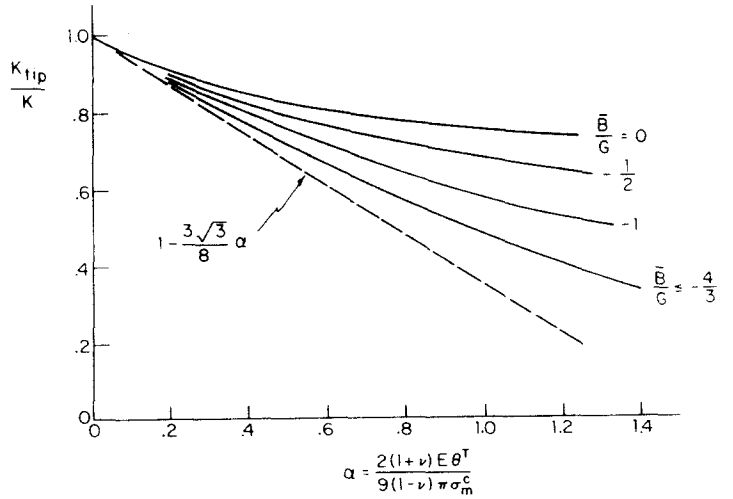

Fig. 8. Ratio of near-tip to remote stress intensity factor. The dashed line is the asymptotic results for small α. The curves for the sub-critically transforming materials ($\bar{B}/G > -4/3$) were calculated with $\nu = 0.3$.

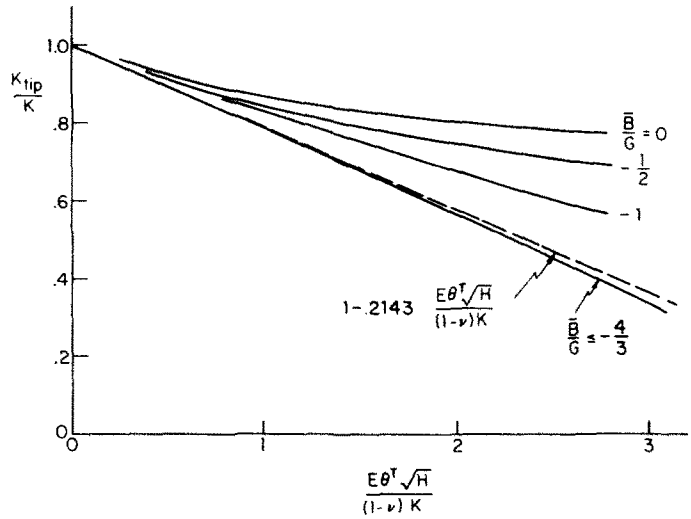

Fig. 9. Ratio of near-tip to remote stress intensity factor. The dashed line is the asymptotic result for small θ^T. The curves for the sub-critically transforming materials were calculated with $\nu = 0.3$.

6. K_{tip} FOR SUB-CRITICALLY TRANSFORMING MATERIALS UNDER STEADY-STATE GROWTH CONDITIONS

An energy balance relation for the plane-strain, steady-state problem is

$$\frac{(1-\nu^2)}{E}K^2 = \frac{(1-\nu^2)}{E}K_{tip}^2 + 2\int_0^H U(x_2)\,dx_2 \tag{43}$$

where $U(x_2)$ is the residual energy density (i.e. residual stress work per unit area per unit thickness in the x_3-direction) left behind in the wake as $x_1 \to -\infty$. In words, (43) states that of the energy released from the remote field per unit crack extension part is deposited in the wake and the remainder is released by the advancing crack tip through the term involving K_{tip}^2. A direct derivation of (43) from the field equations governing the steady-state problem is given in the Appendix.

The residual energy density has two components: a part associated with the transformation and a contribution due to residual stresses, $\sigma_{11}(x_2)$ and $\sigma_{33}(x_2)$, left behind in the wake as $x_1 \to \infty$. The transformational contribution is (refer to Fig. 2) the net work associated with the hysteresis loop leaving a residual dilatation θ at $\sigma_m = 0$. This is

$$\sigma_m{}^c\theta + \frac{\bar{B}\theta^2}{2(1-\bar{B}/B)}. \tag{44}$$

Far downstream in the wake, $\sigma_{22} = 0$ while the constraint of the elastic half-spaces above and below the wake requires $\epsilon_{11} = 0$. From the plane strain relations (19)–(22), one finds that the nonzero stresses in the wake as $x_1 \to -\infty$ are given by

$$\sigma_{11} = \sigma_{33} = -E\theta/(3(1-\nu)) \tag{45}$$

which results in a residual elastic strain energy density of $E\theta^2/(9(1-\nu))$. In terms of the distribution of $\theta(x_2)$ in the wake, the residual energy deposited into the wake per unit crack extension is therefore

$$2\int_0^H U(x_2)\,dx_2 = 2\int_0^H \left\{\sigma_m{}^c\theta + \frac{\bar{B}\theta^2}{2(1-\bar{B}/B)} + \frac{E\theta^2}{9(1-\nu)}\right\}dx_2. \tag{46}$$

The energy balance (43) with (46) provides an alternative expression to (33) for calculating K_{tip} if the distribution of θ is known. Both expressions were used as a consistency check on the

accuracy of our numerical solution. The expression (46) for the residual energy in the wake is limited to $\bar{B} \geq -4G/3$. As discussed in the Appendix, for super-critically transforming materials (43) remains valid if (46) is evaluated using $\bar{B} = -4G/3$. Then

$$2\int_0^H U(x_2)\,dx_2 = 2H\sigma_m^c\theta^T \tag{47}$$

since the full transformation takes place across the wake and the two quadratic terms in θ cancel. In the calculations reported in the previous section for the super-critically transforming materials, (43) with (47) was also used to compute K_{tip}/K. Agreement to within 0.3% of the results calculated using the area integral (33) was found. It is a simple matter to show that the asymptotic results (40) and (41) are retrieved from the energy balance equation when θ^T is small.

The numerical method used for the sub-critically transforming materials was developed for the analogous steady-state elastic–plastic crack growth problem by Dean and Hutchinson[7]. Similar calculations for elastic–plastic solids have also been performed by Parks *et al.*[8] and by Hui[9] and Douglas *et al.*[10] who have extended the method to include viscous and dynamic effects. The method is an iterative one in which estimates of the zone shape and the distribution of θ in any iterative step are used to generate improved estimates in the subsequent step. The steady-state character of the problem enters in that the solution at any point in the zone involves the history of that material point over its path in the negative x_1-direction from its intersection with the leading edge of the zone. In the steady-state problem the dilatation-rate is related to the spatial gradient of the dilatation by

$$\dot{\epsilon}_{pp} = -\dot{a}\,\partial\epsilon_{pp}/\partial x_1 \tag{48}$$

where $\dot{a}$ is the crack growth-rate. Thus, loading occurs in the forward part of the zone in which $\partial\epsilon_{pp}/\partial x_1 < 0$ and unloading occurs in the rear part of the zone (i.e. the wake) whose forward boundary is characterized by $\partial\epsilon_{pp}/\partial x_1 = 0$.

A displacement-based finite element method was used to discretize the field equations as discussed in Ref.[7]. A coarse representation of the finite element grid is shown in Fig. 10. The actual grid contained a total of 2592 quadrilateral elements, each of which was comprised of four constant strain triangular elements. Tractions determined from the remote field (24) were imposed on the outer boundary, whose closest distance to the crack tip was chosen to be about 150 times the half-height H of the transformation zone. A highly refined grid was laid out within a region around the tip. The dimension of the smallest elements was about $H/27$. A total of 17 quadrilateral elements spanned the half-wake in the x_2-direction and 22 elements fell between the crack tip and the leading edge of the zone.

The finite element equations have the general form

$$\mathbf{Mu} = \mathbf{P} - \mathbf{N}\boldsymbol{\theta} \tag{49}$$

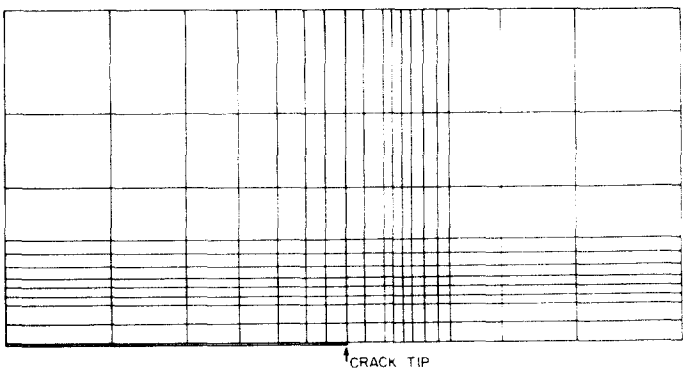

Fig. 10. Coarse layout of finite element grid.

where $\mathbf{M}$ is the elastic stiffness matrix, $\mathbf{u}$ is the nodal displacement vector, $\mathbf{P}$ is the load vector associated with the boundary tractions, and $\mathbf{N}\boldsymbol{\theta}$ is the contribution of the transformed dilatation which enters in the form of a distributed body force. Given an estimate of $\boldsymbol{\theta}$ in any iterative step, (49) was solved for $\mathbf{u}$ and then the next estimate of the total strain in each element was obtained. From this new estimate of the total strain distribution the next estimate of the loading and wake regions of the transformation zone and of $\boldsymbol{\theta}$ was determined. In the loading portion of the zone θ can be expressed directly in terms of ϵ_{pp} according to

$$\begin{aligned} \theta &= 0, && \epsilon_{pp} < \epsilon^c_{pp} \\ &= (1 - B/\bar{B})(\epsilon_{pp} - \epsilon^c_{pp}), && \epsilon^c_{pp} < \epsilon_{pp} < \epsilon^0_{pp} \\ &= \theta^T, && \epsilon^0_{pp} < \epsilon_{pp} \end{aligned} \tag{50}$$

where $\epsilon^c_{pp} \equiv \sigma_m{}^c/B$ and $\epsilon^0_{pp} = \epsilon^c_{pp} + \theta^T(1 - \bar{B}/B)^{-1}$. In the wake θ is independent of x_1, as already discussed, and $\theta(x_2)$ was assigned the value attained at the rear boundary of the loading zone where $\partial\epsilon_{pp}/\partial x_1 = 0$.

The elastic solution with $\boldsymbol{\theta} = 0$ was used to initiate the process. Extremely rapid convergence was obtained, with 7 or 8 iterations sufficient to obtain convergence of computed quantities to three or four significant figures. (This convergence is considerably better than what was found for the corresponding elastic-plastic problem, most likely because it is not possible to write an integrated relation between the plastic strain and the total strain analogous to (50) in the elastic–plastic problem.)

In the small scale transformation problem use of the dimensionless coordinates $x_1(\sigma_m{}^c/K)^2$ and $x_2(\sigma_m{}^c/K)^2$ incorporates all of the dependence on K. The three remaining dimensionless parameters which fully specify the problem are α in (42), $\bar{B}/G$, and Poisson's ratio ν which was taken to be 0.3 in all the calculations reported below. (For the super-critically transforming materials the dependence on ν is all incorporated in α, but ν must be specified independently in the calculations for the sub-critically transforming materials. As already seen, one solution applies to all the super-critically transforming materials, as it is independent of $\bar{B}/G$.)

Plots of the transformed dilatation θ ahead of the crack tip ($x_1 > 0$, $x_2 = 0$) are shown in Fig. 11 for various values of α for the case $\bar{B} = 0$. Two normalizations of θ have been used in these plots: θ/θ^T in Fig. 11(a) and in Fig. 11(b) we used θ/ϵ^c_{pp} where $\epsilon^c_{pp} \equiv \sigma_m{}^c/B$ is the elastic dilatation at the onset of the transformation. Similar plots of the distributions $\theta(x_2)$ across the wake are shown in Fig. 12. From Figs. 11(a) and 12(a) it is seen that only a relatively small portion of the zone is fully transformed (i.e. $\theta = \theta^T$) when α is not small. However in the mathematical limit $\alpha \to 0$, the entire zone becomes fully transformed and the zone boundary is described by (37)–(39). The normalization used in Figs. 11(b) and 12(b) brings out the fact that the θ-distribution is essentially independent of θ^T in the partially transformed zone where $\theta < \theta^T$ until full transformation is achieved. Similar distributions were found for $\bar{B}/G = -1/2$ and $\bar{B}/G = -1$. However, for a fixed value of α, the portion of the zone which is partially transformed shrinks as $\bar{B}/G$ becomes more negative and must vanish as $\bar{B} \to -4G/3$.

Plots of $\sigma_m/\sigma_m{}^c$ and $\sigma_{22}/\sigma_m{}^c$ ahead of the crack tip are displayed in Fig. 13, again for various α with $\bar{B} = 0$.

Curves of K_{tip}/K as a function of α and $E\theta^T\sqrt{(H)}/[(1-\nu)K]$ have been included in Figs. 8 and 9, respectively, for $\bar{B}/G = 0$, $-1/2$ and -1. The results shown were computed by means of the area integral (33). (Analytic integration around the crack tip was performed to take care of the singularity at the tip.) The energy balance relation (43) was also used to compute K_{tip}/K. The discrepancy between the two computed values of $(K_{tip}/K - 1)$ was less than 3% when α was less than 0.5 and was less than 7% when $\alpha = 1$. As expected, the sub-critically transforming materials give rise to smaller reductions in the near-tip intensity factor than the super-critically transforming materials primarily because much of the zone is only partially transformed.

7. DISCUSSION

Our analysis has assumed that the transformation zone spans many particles so that a continuum description of the composite material could be invoked. Use of the near-tip stress intensity factor to characterize the intensity level in the fracture process zone is likewise only

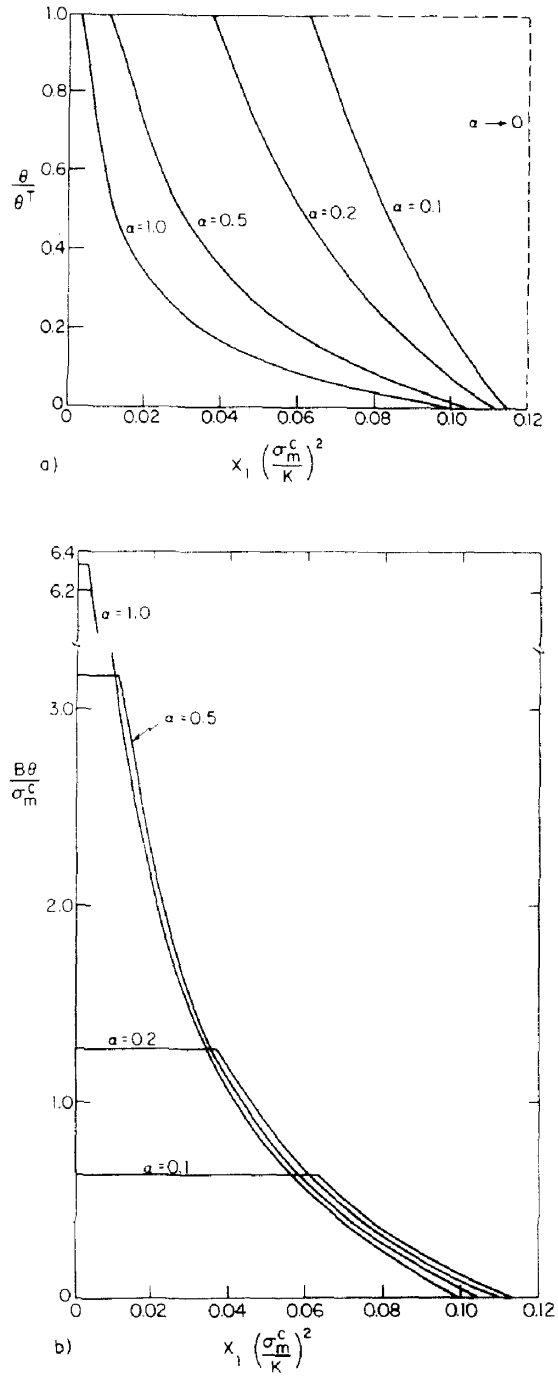

Fig. 11. Distribution of transformed dilatation ahead of crack tip for various α with $\bar{B} = 0$.

meaningful if the dominant region of the K_{tip}-field spans this process zone. Possible effects of interactions between the crack-front and individual particles, such as crack trapping at local points along the front, have not been considered.

The theoretical predictions for toughening enhancement based on the reduction of K_{tip} below the applied K depend strongly on whether the composite material transforms in a super- or sub-critical manner. In Fig. 9 it is seen that the implied increase in toughness given by the asymptotic equation (40), i.e.

$$\Delta K \equiv K - K_{tip} = 0.2143 \frac{Ec\theta_p^T}{(1-\nu)} \sqrt{(H)} \tag{51}$$

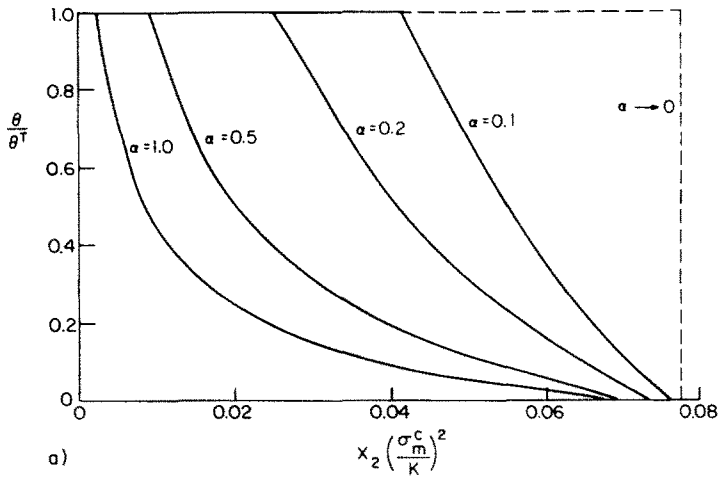

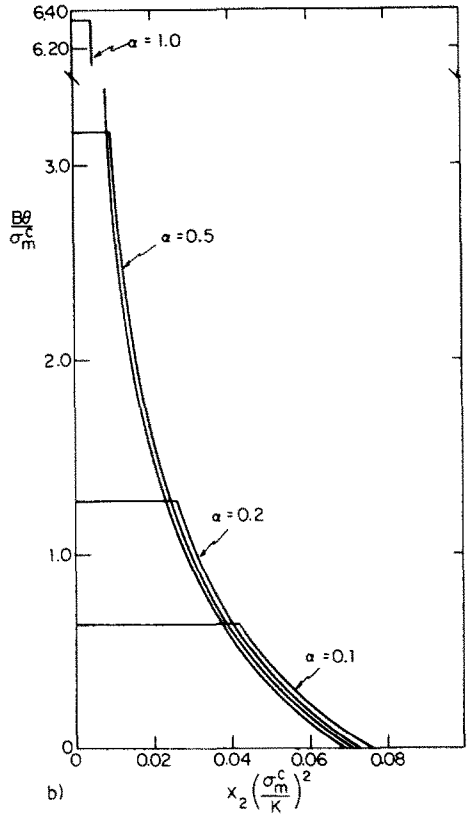

Fig. 12. Distribution of transformed dilatation across the wake for various α with $\bar{B} = 0$.

holds accurately for the super-critically transforming materials over the full range of interest. Values of ΔK for the sub-critically transforming materials can be substantially less. For example, from Fig. 9, it can be seen that when $\Delta K/K = 0.5$ for the super-critical materials it is only about 0.25 for the corresponding sub-critical material with $\bar{B} = 0$. Assignment of values to $\bar{B}/G$ based on experimental data is not yet possible; and, indeed, a particular value is expected to depend on the distribution of particle sizes, as discussed previously.

A tentative comparison of eqn (51) for ΔK with three sets of experimental data is possible.† First, McMeeking and Evans[2] compared (51) with data of Porter and Heuer[11] and

†We are indebted to A. G. Evans for supplying this data.

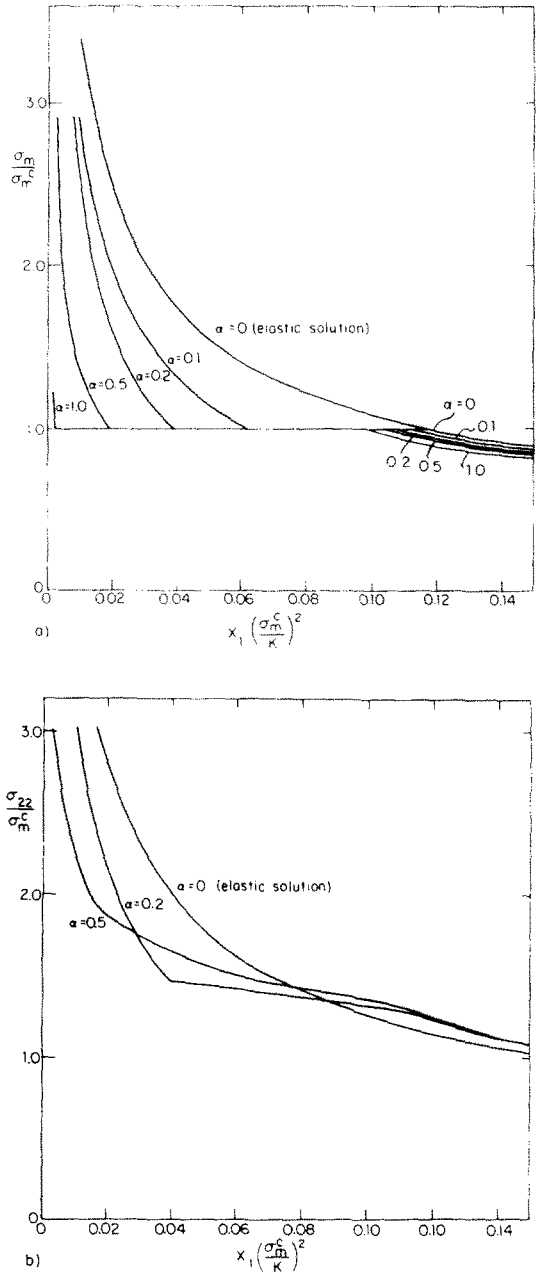

Fig. 13. Mean stress and normal stress ahead of crack tip for various α with $\bar{B} = 0$.

Schoenlein[12] for a two phase zirconia system. The data used for this system was $E = 200$ GPa, $c = 0.3$, $\theta_p{}^T = 0.058$ and $H = 0.6\,\mu$m. The measured increase in fracture toughness was about $\Delta K = 2.3$ MN/m$^{3/2}$. Equation (51) predicts $\Delta K = 0.81$ MN/m$^{3/2}$ with $\nu = 0.29$. Another two-phase zirconia system was studied by Swain[13], and for this system $E = 170$ GPa, $c = 0.3$, $\theta_p{}^T = 0.04$ and $H \cong 1\ \mu$m with a measured toughness increase of $\Delta K = 2$ MN/m$^{3/2}$. For this system the theoretical toughness increase from (51) is $\Delta K = 0.62$ MN/m$^{3/2}$. The third system studied by Claussen and Rühle[14], has zirconia particles in an alumina matrix. For this system $E = 470$ GPa, $c = 0.3$, $\theta_p{}^T = 0.04$ and $H \cong 5\ \mu$m. The measured increase in toughness is about $\Delta K = 6$ MN/m$^{3/2}$, while (51) predicts $\Delta K = 3.8$ MN/m$^{3/2}$.

These comparisons must be regarded as tentative since the experimental measurements are difficult and some of the assigned parameter values may be questionable. Nevertheless, in each of the above comparisons the theoretical prediction based on the super-critically transforming

material accounts for only about one-third to two-thirds of the observed increase in toughening. Since the super-critically transforming material gives the largest predicted increase, it seems reasonable to conclude that distortional as well as dilatant components of transformation, together with possible preferred orientation effects may have to be taken into account along with the dilatant component.

Acknowledgements—Our interest in this problem area was first stimulated by A. G. Evans. Throughout the course of the work he served both as a source of ideas and information and as a critic. We are also indebted to helpful conversations with R. M. Cannon about the range of possible composite transformation behaviors, and with R. D. James about the path-independence of the J-integral when discontinuities in the stress and strain fields occur. The work was initiated in the summer of 1980 under the auspices of the Defense Advanced Research Projects Agency under contract MDA903-80-C-0505 with the University of Michigan. It was completed in part with the support of the National Science Foundation under grants DMR-80-20247 and CME-78-10756, and by the Division of Applied Sciences, Harvard University.

REFERENCES

1. A. G. Evans and A. H. Heuer, Transformation toughening in ceramics: martensitic transformations in crack-tip stress fields. *J. Am. Ceram. Soc.* **63**, 241–248 (1980).
2. R. M. McMeeking and A. G. Evans, Mechanics of transformation toughening in brittle materials *J. Am. Ceram. Soc.* **65**, 242–246 (1982).
3. R. Hill, Elastic properties of reinforced solids: some theoretical principles. *J. Mech. Phys. Solids* **11**, 357–372 (1963).
4. F. R. N. Nabarro, The strains produced by precipitation in alloys. *Proc. Roy. Soc. Lond. A* **175**, 519–538 (1940).
5. J. R. Rice, Mathematical analysis in the mechanics of fracture. In *Fracture* (Edited by H. Liebowitz), Vol. 2, pp. 191–311. Academic Press, New York (1968).
6. J. W. Hutchinson, On steady quasi-static crack growth. Harvard University Rep. Division of Applied Sciences, DEAP S-8, April 1974.
7. R. H. Dean and J. W. Hutchinson, Quasi-static steady crack growth in small scale yielding. In *Fracture Mechanics*, ASTM-STP 700, pp. 383–405 (1980).
8. D. M. Parks, P. S. Lam and R. M. McMeeking, Some effects of inelastic constitutive models on crack tip fields in steady quasistatic growth. In *Advances in Fracture Research* (Edited by D. Francois), Vol. 5, pp. 2607–2614 (1981).
9. C. Y. Hui, Steady state crack growth in elastic power-law creeping materials. Harvard University Rep. Division of Applied Science, MECH-21, Aug. 1981.
10. A. S. Douglas, L. B. Freund and D. M. Parks, Dynamic steady antiplane shear crack growth in an elastic-plastic material. In *Advances in Fracture Research* (Edited by D. Francois), Vol. 5, pp. 2233–2240 (1981).
11. D. L. Porter and A. H. Heuer, Mechanisms of toughening partially stabilized zirconia (PSZ). *J. Am. Ceram. Soc.* **60**, 183–184 (1977).
12. L. Schoenlein, M.S. Thesis, Case Western Reserve University (1979).
13. M. Swain, Private communication of work to be published through A. G. Evans.
14. N. Claussen and M. Rühle, Private communicatiuon of work to be published through A. G. Evans.
15. A. C. Palmer and J. R. Rice, The growth of slip surfaces in the progressive failure of over-consolidated clay. *Proc. Roy. Soc. Lond. A* **332**, 527–548 (1973).

APPENDIX

Analysis of the steady-state problem for the super-critically transforming material

With reference to Fig. 4, let $z = x_1 + ix_2$ be the complex variable denoting a point at (x_1, x_2) and let $z_0 = x_1^0 + ix_2^0$ be the point at the center of the circular spot located above the x_1-axis. The mean stress at any point z outside the two spots is [6]

$$\sigma_m = \frac{2(1+\nu)E\theta b^2}{9(1-\nu)} \operatorname{Re}\{g(z, z_0) + g^*(z, z_0)\} \tag{52}$$

where Re denotes the real part,

$$g(z, z_0) = -\frac{1}{2}\frac{1}{(z-z_0)^2} + \frac{1}{4}\frac{1}{z_0}\sqrt{\left(\frac{z_0}{z}\right)}\frac{(z+z_0)}{(z-z_0)^2}$$

and $g^*(z, z_0) \equiv \overline{g(\bar{z}, z_0)}$, with $\bar{(\ )}$ denoting complex conjugation. The steady-state problem posed in Fig. 6 requires that σ_m approach σ_m^c as the boundary of the leading edge of the transformation zone is approached from the outside. By superposition, (52) and (35) imply that the leading edge of the boundary is governed by

$$(L/R(\phi))^{1/2}\cos(\phi/2) + \alpha\iint_A \operatorname{Re}\{g(z, z_0) + g^*(z, z_0)\}\,dx_1^0\,dx_2^0 = 1 \tag{53}$$

$$0 \le \phi \le \phi_0$$

where $L = (2(1+\nu)^2/9\pi)(K/\sigma_m^c)^2$. α is given in (42) and $z = R(\phi)(\cos\phi + i\sin\phi)$. It is possible to reduce (53) further by carrying out the integration with respect to x_1^0 (with x_2^0 fixed) from $-\infty$ to the leading edge of the zone boundary. That step gives the integral equations for $R(\phi)$ as

$$(L/R(\phi))^{1/2}\cos(\phi/2) + \alpha\int_0^{\phi_0} F(\phi, \bar{\phi})\,d\bar{\phi} = 1 \qquad 0 \le \phi \le \phi_0 \tag{54}$$

where

$$F(\phi,\bar{\phi})=\frac{1}{2}\,\mathrm{Re}\{(z_0-z)^{-1}[1-(z_0/z)^{1/2}]+(\bar{z}_0-z)^{-1}[1-(\bar{z}_0/z)^{1/2}]\}\frac{\mathrm{d}}{\mathrm{d}\bar{\phi}}(R(\bar{\phi})\sin\bar{\phi})$$

with $z=R(\phi)(\cos\phi+i\sin\phi)$ and $z_0=R(\bar{\phi})(\cos\bar{\phi}+i\sin\bar{\phi})$.

At this point ϕ_0 is not known. However, a separate calculation, which we omit, shows that there cannot be a corner where the wake boundary ($x_2=H$) joins the leading edge boundary at $\phi=\phi_0$. That is, R must satisfy

$$\frac{\mathrm{d}}{\mathrm{d}\phi}(R\sin\phi)=0 \quad \text{as} \quad \phi\to\phi_0 \tag{55}$$

ensuring that the leading-edge boundary has a horizontal tangent at ϕ_0. This condition together with (54) determines both ϕ_0 and $R(\phi)$ in $(0,\phi_0)$.

An approximate solution for $R(\phi)$ and ϕ_0 was obtained as follows. A series expression for $R(\phi)$ was written as

$$R(\phi)\sin\phi=\sum_{k=1}^{N}A_k\sin\left(\left(k-\frac{1}{2}\right)\pi\phi/\phi_0\right)\qquad 0\le\phi\le\phi_0 \tag{56}$$

where the A_k's (and ϕ_0) are the new unknowns. Condition (55) is satisfied by (56). For any given set of A_k's and ϕ_0 the l.h.s. of (54) is a well defined function of ϕ; denote it by $Q(\phi)$. With

$$V(A_1,A_2,\ldots,A_N,\phi_0)\equiv\int_0^{\phi_0}[Q(\phi)-1]^2\,\mathrm{d}\phi \tag{57}$$

the integral equation (54) was replaced by the problem of minimizing V with respect to A_1 through A_N and ϕ_0. (Of course, the trivial minimum with $\phi_0=0$ is excluded.) The minimization process was carried out by means of a numerically implemented Newton–Raphson method. Solutions were generated with $N=1$, $N=2$ and $N=3$. The predominant term is that associated with A_1; the quantities H and K_{tip}/K were obtained to within 1% with just $N=1$. The θ-variation associated with A_1 is not exactly the elastic solution (38), but is very close to it. As mentioned in the body of the paper, (38) with H given by Fig. 7 gives an excellen approximation to the boundary of the zone. The angle ϕ_0 increases from 60° for $\alpha=0$ to 61.5° for $\alpha=0.5$ to 64.1° for $\alpha=1$.

For the super-critical case with $\theta=\theta^T$ the double integral in (33) can be reduced to an integral along the leading edge of the zone by performing the integration with respect to x_1 with x_2 held fixed. The result can be written as

$$K_{\mathrm{tip}}/K=1-\alpha\int_0^{\phi_0}\cos(\phi/2)R(\phi)^{-1/2}\frac{\mathrm{d}}{\mathrm{d}\phi}(R\sin\phi)\,\mathrm{d}\phi. \tag{58}$$

Derivation of energy balance for steady-state problem

A derivation of energy balance in steady-state elastic–plastic crack growth was given in Ref. [6]. The same derivation actually applies to the present problem with phase transformation but a brief recapitulation of the analysis will be given here. Let U be the stress work density at any material point defined by

$$U(\boldsymbol{\epsilon},\text{history})=\int_0^{\boldsymbol{\epsilon}}\sigma_{ij}\,\mathrm{d}\epsilon_{ij} \tag{59}$$

while it is assumed that there is no initial spatial variation in material properties, U is a history dependent function in that the linear unloading response of the material is *not* suppressed. For plane deformations under steady-state growth conditions, the following line integral will be shown to be path-independent:

$$I=\int_\Gamma(Un_1-\sigma_{ij}n_ju_{i,1})\,\mathrm{d}s \tag{60}$$

where the crack is taken to be aligned with the x_1-axis and Γ is a contour such as that in Fig. 3. As emphasized in Refs. [6] and [15], this reduces to the well known J-integral for small strain nonlinear elastic (deformation theory) materials; for the irreversible behavior of interest here path-independence holds only in the steady state.

To prove path independence, let C be any closed contour in the x_1-x_2 plane, let the region A_C within C contain no singularities, and let $\mathbf{n}$ be the outward unit normal to C. By the divergence theorem

$$\int_C Un_1\,\mathrm{d}s=\int_{A_C}U_{,1}\,\mathrm{d}A=-\int_{A_C}\frac{\partial U}{\partial a}\,\mathrm{d}A. \tag{61}$$

The last equality in (61) follows from the relation between partial derivatives

$$\partial(\ )/\partial a=-\partial(\ )/\partial x_1 \tag{62}$$

which holds for steady-state growth in the x_1-direction. It is to be understood that $\partial(\ )/\partial a$ denotes the derivative with respect to crack advance at a fixed material point and $\partial(\ )/\partial x_1$ denotes differentiation with the crack length a held fixed. Continuing with (61), we can write

$$-\int_{A_C}\frac{\partial U}{\partial a}\,\mathrm{d}A=-\int_{A_C}\sigma_{ij}\frac{\partial\epsilon_{ij}}{\partial a}\,\mathrm{d}A=\int_{A_C}\sigma_{ij}\epsilon_{ij,1}\,\mathrm{d}A.$$

$$=\int_{A_C}(\sigma_{ij}u_{i,1})_{,j}\,\mathrm{d}A=\int_C\sigma_{ij}n_ju_{i,1}\,\mathrm{d}s. \tag{63}$$

The first step in the above continued equality is permissible because the derivative of U is taken at a fixed material point. The second step again uses (62), while the remaining steps use equilibrium and the divergence theorem. Thus, by (61) and (63),

$$\int_C (Un_1 - \sigma_{ij} n_j u_{i,1})\, ds = 0.$$

Since the integrand of I in (60) vanishes on the crack faces, it therefore follows that I has the same value for all contours Γ encircling the tip.

Since (26) holds at the crack tip, by shrinking Γ down to the tip one finds (for plane strain)

$$I = (1 - \nu^2) K_{\text{tip}}^2 / E. \tag{64}$$

Next take Γ as a circular contour of radius R which is very large compared to the zone height. On this contour there are two contributions to I; one from the remote field (24) outside the wake and the other from the wake itself. Imagining $R \to \infty$, one finds

$$I = (1 - \nu^2) K^2 / E - 2 \int_0^H U(x_2)\, dx_2 \tag{65}$$

where $U(x_2) = \lim_{x_1 \to -\infty} U(x_1, x_2)$. The term $\sigma_{ij} n_j u_{i,1}$ vanishes in the remote wake. Taken together, (64) and (65) give the energy balance (43) introduced earlier. The above derivation of the path-independence of I requires continuity of the stress and strain fields and thus is limited to the sub-critically transforming materials, although it does apply in the limit $\bar{B} = -4G/3$ for the critically transforming material. For the super-critically transforming materials ($\bar{B} < -4G/3$), the transformation no longer occurs quasi-statically. We have not attempted to write a general energy balance relation for the super-critically transforming materials. However, since the energy balance (43) does apply to the case $\bar{B} = -4G/3$ and since the solution for all the super-critically transforming materials is the same as that for $\bar{B} = -4G/3$, it follows that (43) holds for the super-critical material when U is evaluated using $\bar{B} = -4G/3$.